SANDIA REPORT
SAND2006-6923
Unlimited Release
Printed November 2006

Engineering intracellular active transport systems as *in vivo* biomolecular tools

George D. Bachand and Amanda Carroll-Portillo

Prepared by
Sandia National Laboratories
Albuquerque, New Mexico 87185 and Livermore, California 94550

Sandia is a multiprogram laboratory operated by Sandia Corporation,
a Lockheed Martin Company, for the United States Department of Energy's
National Nuclear Security Administration under Contract DE-AC04-94AL85000.

Issued by Sandia National Laboratories, operated for the United States Department of Energy by Sandia Corporation.

Available to DOE and DOE contractors from
U.S. Department of Energy
Office of Scientific and Technical Information
P.O. Box 62
Oak Ridge, TN 37831

Telephone: (865)576-8401
Facsimile: (865)576-5728
E-Mail: reports@adonis.osti.gov
Online ordering: http://www.osti.gov/bridge

Available to the public from
U.S. Department of Commerce
National Technical Information Service
5285 Port Royal Rd
Springfield, VA 22161

Telephone: (800)553-6847
Facsimile: (703)605-6900
E-Mail: orders@ntis.fedworld.gov
Online order: http://www.ntis.gov/help/ordermethods.asp?loc=7-4-0#online

SAND2006-6923
Unlimited Release
Printed November 2006

Engineering intracellular active transport systems as in vivo biomolecular tools

George D. Bachand and Amanda Carroll-Portillo
Biomolecular Interfaces and Systems Department

Sandia National Laboratories
P.O. Box 5800, MS1413
Albuquerque, NM 87185-1413

Abstract

Active transport systems provide essential functions in terms of cell physiology and metastasis. These systems, however, are also co-opted by invading viruses, enabling directed transport of the virus to and from the cell's nucleus (i.e., the site of virus replication). Based on this concept, fundamentally new approaches for interrogating and manipulating the inner workings of living cells may be achievable by co-opting Nature's active transport systems as an *in vivo* biomolecular tool. The overall goal of this project was to investigate the ability to engineer kinesin-based transport systems for *in vivo* applications, specifically the collection of effector proteins (e.g., transcriptional regulators) within single cells. In the first part of this project, a chimeric fusion protein consisting of kinesin and a single chain variable fragment (scFv) of an antibody was successfully produced through a recombinant expression system. The kinesin-scFv retained both catalytic and antigenic functionality, enabling selective capture and transport of target antigens. The incorporation of a rabbit IgG-specific scFv into the kinesin established a generalized system for functionalizing kinesin with a wide range of target-selective antibodies raised in rabbits. The second objective was to develop methods of isolating the intact microtubule network from live cells as a platform for evaluating kinesin-based transport within the cytoskeletal architecture of a cell. Successful isolation of intact microtubule networks from two distinct cell types was demonstrated using glutaraldehyde and methanol fixation methods. This work provides a platform for inferring the ability of kinesin-scFv to function *in vivo*, and may also serve as a three-dimensional scaffold for evaluating and exploiting kinesin-based transport for nanotechnological applications. Overall, the technology developed in this project

represents a first-step in engineering active transport system for *in vivo* applications. Further development could potentially enable selective capture of intracellular antigens, targeted delivery of therapeutic agents, or disruption of the transport systems and consequently the infection and pathogenesis cycle of biothreat agents.

Acknowledgments

This work was supported by Sandia's Laboratory Directed Research and Development (LDRD) Project 79887. Sandia is a multiprogram laboratory operated by Sandia Corporation, a Lockheed Martin Company, for the United States Department of Energy under Contract DE-AC04-94AL85000.

Table of Contents

Intentionally Left Blank

1.0 Introduction

Active transport systems have evolved as Nature's means of alleviating diffusional constraints, specifically with relation to moving large macromolecules within the gel-like environment of the cytoplasm [1]. For example, diffusion of a 30-nm vesicle to a location 3-μm away in the cytoplasm would require ~540 seconds. Alternatively, active transport of this vesicle across the same distance occurs in less than 5 seconds, a two-order of magnitude difference. Active transport systems are composed of filament networks that serve as tracks on which motor proteins drive the directed transport of cargo through the efficient conversion of chemical energy into mechanical work. These systems are ubiquitous in living organisms, and are fundamental to a wide range of physiological process including cell division, chromosome segregation, vesicle trafficking, and muscle actuation [2-6].

The cytoskeleton provides structural integrity to the cell, but also functions an intricate, three-dimensional network for active transport systems. Cytoskeletal filaments are classified into three distinct types: (*i.*) actin filaments, (*ii.*) intermediate filaments, and (*iii.*) microtubule filaments. Actin and microtubule filaments serve primarily as "molecular tracks" within the cell, while intermediate filaments function only as structural elements that reinforce the cell and help organize cells into tissues [4]. Motor proteins responsible for moving macromolecules along actin and microtubule filaments are also sub-divided into three types: myosin, kinesin, and dynein. The myosin family of motor proteins works in conjunction with actin filaments to facilitate contraction of muscle cells, as well as transport intracellular vesicles [5, 7]. Dynein and kinesin motor proteins are involved in bi-directional trafficking of macromolecular cargo on microtubule filaments [3, 7]. Dynein and kinesin are responsible for a wide array of functions including vesicle transport [8-10], the color changing mechanisms common in fish [11-13], cilia actuation [14], mitotic spindle assembly [15, 16], and lipid tubule formation in the endoplasmic reticulum [17].

The kinesin family of motor proteins contains fourteen sub-families in which distinct structural features and physiological roles may be assigned. Of these sub-families, Kinesin-1, often referred to as conventional kinesin, has been the most intensely studied. Conventional kinesins are homo-dimer proteins that possess three structural domains: a motor domain, a neck-linker region, and an α-helical, coiled-coil tail region [1-3, 7]. The biochemical and biophysical properties of conventional kinesin have been well-characterized. Conventional kinesin moves processively (i.e., repetitively stepping without dissociating from the microtubule) from the minus-end to the plus-end of the microtubule filament through an asymmetric hand-over-hand mechanism [18-21]. Each 8-nm step requires the hydrolysis of a single ATP molecule, and produces ~40 pN·nm mechanical work with an overall catalytic efficiency of ~50% [20-24]. As a whole, kinesin motor proteins represent a class of biological molecular motors crucial to the intracellular transport of macromolecules within the nanofluidic environment of a cell.

The potential application of kinesin-based transport in nanoscale systems was recognized over 7 years ago [25], and has driven multi-disciplinary efforts focused on integrating these molecular motors as nanoscale actuators in hybrid systems [26-30].

Reconstitution of the kinesin-microtubules in synthetic systems can be achieved in two different geometries [28, 30]. In the first geometry, microtubule filaments are bound to a positively charged surface (e.g., amine-terminated self-assembled monolayer), and serve as the tracks for kinesin movement; this geometry directly mimics the natural system. The second geometry involves the formation of a kinesin monolayer with the motor domains extending into the solution, and the collective movement of microtubules across a surface; this geometry is known as the gliding or inverted geometry. The majority of work in applying kinesin and microtubules to nanoscale systems has focused on the gliding motility geometry as a "molecular shuttle" for moving nanoparticles and materials [28, 30].

2.0 General Strategy

Viruses and some bacteria are able to co-opt active transport systems to facilitate efficient transport within the cell's cytoplasm [31-36]. For example, the infection cycle of Vaccinia virus requires microtubule-based transport of intracellular mature and extracellular enveloped forms of the virus within the cell [37, 38]. Other viruses, such as herpes simplex viruses, require microtubule-based transport of virions to the nucleus of the cell, where replication occurs, and back to the cell membrane to initiate cell-to-cell spread [39-42]. This ability of viruses to co-opt the cell's active transport system raises an interesting question: can such intracellular transport systems be co-opted for directed *in vivo* manipulations? Specific manipulations may include collection of proteins and small molecules within individual cells, disrupting virus/bacterium infection cycles, directing the transport of effector molecules for localized stimulation, or the delivery of therapeutic agents to specific sites within a cell.

The overall goal of this project was to investigate the ability to engineer kinesin-based transport systems for *in vivo* applications, specifically the collection of effectors (e.g., transcriptional regulators) within single cells. The objectives of this work included (*i.*) engineering an analyte-selective kinesin motor protein, (*ii.*) characterizing the antigenic and catalytic properties of the analyte-selective kinesin, and (*iii.*) developing methods to harvest intact microtubule supra-structures from live cells. The following report summarizes the achievements of this one-year project.

3.0 Engineering and characterizing analyte-selective kinesin motors proteins

Directed *in vivo* manipulation of kinesin-based transport systems necessitates the development of engineered kinesin motor proteins with target-selective features. Thus, the first critical milestone of this work was engineering kinesin motor proteins with an integrated analyte-selective receptor. To achieve this goal, genetic engineering was utilized to fuse an antibody fragment, called a single chain variable fragment (scFv), to the tail region of conventional kinesin. The selectivity and binding affinity of the scFv for the target antigen, however, can be adversely affected when bound to surfaces [43] or

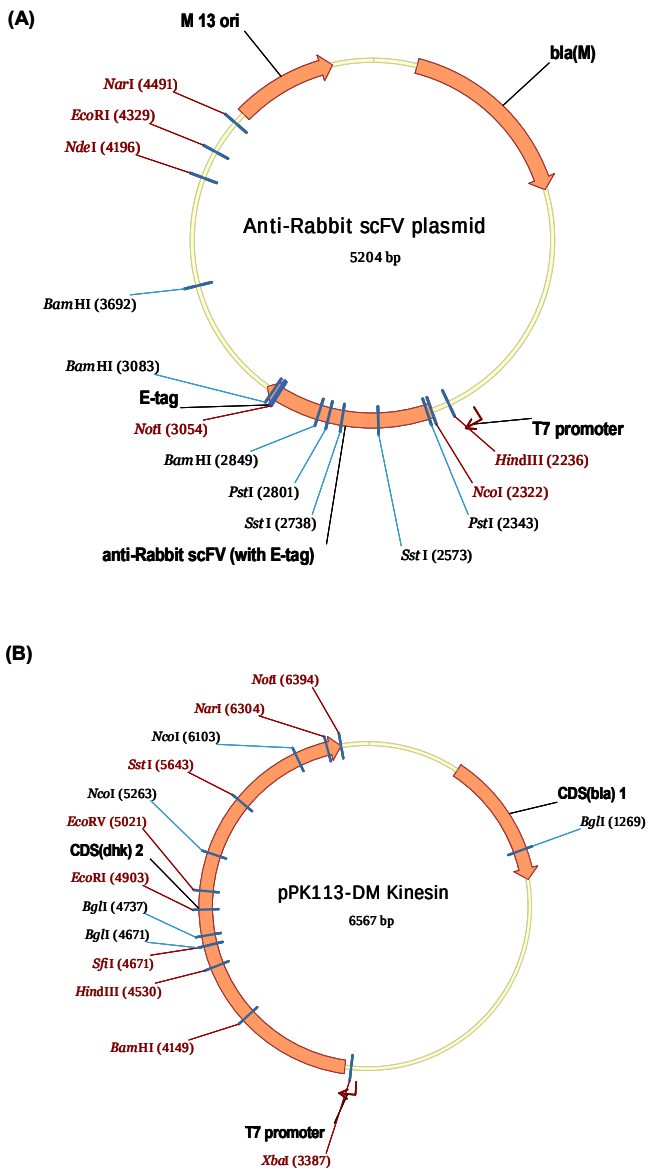

Figure 1. Plasmid maps of the (**A**) anti-rabbit immuglobulin G, single chain variable fragment, and (**B**) pPK113 *Drosophila* kinesin that were used to construct the fusion protein.

other proteins [44]. Therefore, a significant challenge of this work was the development of a kinesin-scFv with proper structural and functional features.

Materials & Methods

Genetic engineering of the kinesin-scFv

A recombinant DNA plasmid containing a scFv specific to rabbit immunoglobulin G (IgG) was graciously provided by Professor Ray Mernaugh of Vanderbilt University (Fig. 1A). Site directed mutagenesis (SDM) was used to genetically modify the scFv sequence

to introduce a *Nar* I restriction endonuclease site to facilitate the insertion of the scFv fragment into the kinesin expression system. Briefly, synthetic oligonucleotides sequences containing the mutated DNA region were synthesized by Sigma-Genosys, and used to generate the mutated plasmid through a variation of the polymerase chain reaction. The DNA lacking the mutation was then removed by restriction endonuclease digestion with *Dpn* I at 37°C for 60 min. The mutated plasmid was then transformed into XL-1 Blue cells (Strategene, Inc.), and characterized by restriction digests and DNA sequencing (Northwoods DNA, Inc).

To construct the kinesin-scFv fusion protein, the modified scFv sequence and *Drosophila* kinesin sequence (pPK113-DM) were excised by digestion with *Nar* I and *Not* I restriction endonucleases (Fig. 1). This digestion removed a small portion of the kinesin tail from pPK113-DM, and the entire anti-rabbit IgG scFv sequence. The scFv and *Drosophila* kinesin fragments were then ligated together using the compatible, sticky ends, and transformed into XL-1 Blue cells. The resulting kinesin-scFv plasmid contained a codon frameshift that was rectified by deleting a thymidine residue at the 5' end of the scFv using SDM. Finally, a 10x His tag and hard stop codon (TAA) were introduced to provide an easy means for protein purification and proper protein length, respectively. DNA sequencing of the final construct was performed by Northwoods DNA, Inc., and analyzed to ensure proper placement and orientation of the individual regions. The final kinesin-scFv plasmid was then transformed into Rosetta®2 DE3 pLysS cells for expression of the recombinant fusion protein. Cells were grown in Lauria-Bertani (LB) media supplemented with ampicillin and chloramphenicol for approximately 4 hrs at 37ºC, induced to express the recombinant protein with isopropyl-beta-D-thiogalactopyranoside (IPTG), and grown for an additional 4 hrs at 23ºC. Cells were collected by centrifugation, and lysed with BugBuster® (Novagen) to release the recombinant protein. The kinesin-scFv was purified by Ni-NTA affinity chromatography, and stored in small aliquots at -85ºC.

Characterization of the recombinant kinesin-scFv

The ATP hydrolytic properties of the kinesin-scFv were characterized using a NADH-coupled double enzyme assay [45]. The kinesin-scFv was diluted to a final concentration of 0.1 μM in the ATP hydrolysis assay buffer (50 mM Tris-acetate, pH 7.5, 1 mM $MgCl_2$, 1 mM dithiotheritol, 1 μM taxol, 1 mM MgATP, 3 mM phosphoenol-pyruvate, 200 μM NADH, and 18 units/mL lactate dehydrogenase, and 12 units/mL pyruvate kinase). The addition of polymerized microtubules at a 0.5 μM concentration was used to stimulate ATP hydrolysis, which was monitored by measuring the absorbance of NADH at 340 nm on a UV-Vis spectrophotometer. ATP hydrolytic rates were determined by linear regression of the absorbance measurements at 340 nm as a function of time using SigmaStat.

The antigenic properties of the kinesin-scFv were characterized using two modified enzyme-linked immunosorbent assays (ELISA). In the first assay, the efficacy of antigen binding to the kinesin-scFv was measured. Microtiter plates were coated with anti-kinesin antibodies at 37ºC for 3 hrs, washed with phosphate-buffered saline with 0.05% Tween-20 (PBS-T) and allowed to bind the kinesin-scFv at 37ºC for 1 hr. Dilutions of an alkaline

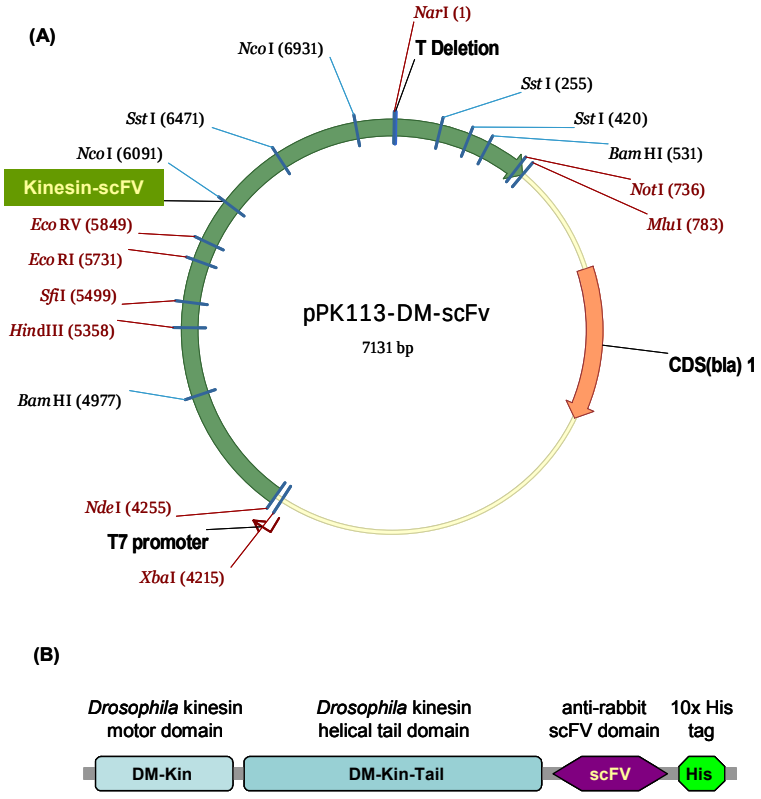

Figure 2: (**A**) Map of the final kinesin-scFv expression plasmid. The anti-rabbit scFv was inserted into the pPK113 *Drosophila* kinesin expression plasmid, immediately downstream of the kinesin sequence, and terminated with a 10x His-tag. (**B**) Schematic diagram of the kinesin-scFv fusion construct showing the location of the different protein domains.

phosphatase-conjugated rabbit IgG were then added and allowed to bind for 1 hr at 37ºC. The substrate, p-nitrophenyl phosphate (pNPP) when then added, and the absorbance at 405 nm was measured approximately 30 min after addition of the substrate. In the second assay, both the antigenic binding and kinesin adhesion to microtubules was measured. Microtiter plates were first coated with anti-tubulin antibodies at 37ºC for 3 hrs, washed with PBS-T, and allowed to bind polymerized, taxol-stabilized microtubules at 37ºC for 1 hr. The kinesin-scFv was then introduced and allowed to bind to the microtubules for 1 hr at 37ºC. Finally, dilutions of an alkaline phosphatase-conjugated rabbit IgG, allowed to bind for 1 hr at 37ºC, and the absorbance at 405 nm was measured approximately 30 min after addition of pNPP. One-way analysis of variance (ANOVA) was used to determine significant differences in the absorbance at 405 nm as a function of alkaline phosphatase-conjugated rabbit IgG concentration.

Results & Discussion

The final plasmid construct, pPK113-DM-scFV, contained a 3657 bp sequence encoding the *Drosophila* kinesin-scFv fusion gene (Fig. 2A), which may be induced to

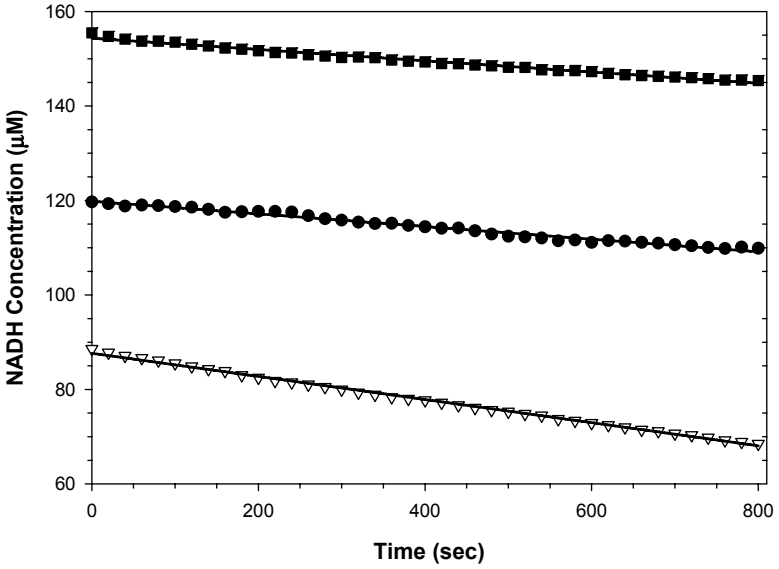

Figure 3. ATP hydrolytic activity of two preparations of the kinesin-scFv, and the native *Drosophila* kinesin. Turnover rates for the kinesin-scFV were estimated at 0.13 (-■-) and 0.25 (-∇-) sec^{-1}; the turnover rate of the native kinesin control was estimated at 0.12 sec^{-1} (-●-). Turnover rates were determined using linear regression analysis.

express recombinant protein through the T7 promotor directly upstream. DNA sequencing results confirmed the correct ordering of the individual domains in the gene sequence. This gene expressed a 1218-amino acid protein that included the kinesin motor domain, the kinesin coiled-coil tail, the anti-rabbit IgG scFv, and a 10x His tag (Fig. 2B). The purified protein had an estimated molecular weight of ~140 kDa based on SDS-PAGE analysis (*not shown*), which is consistent with the predicted molecular weight of the primary amino acid sequence.

The kinesin-scFv displayed microtubule-stimulated ATP hydrolysis, confirming the functionality of the kinesin motor domain (Fig. 3). The relative turnover rate of two kinesin-scFv preparations was estimated at 0.13 (R^2=0.99) and 0.25 sec^{-1} (R^2=0.99), similar to the estimated rate of 0.12 sec^{-1} for the native *Drosophila* kinesin (R^2=0.99; Fig. 3). These ATP hydrolytic rates, however, are significantly lower than published reports for *Drosophila* kinesin [22], and are likely attributed to denaturation of the kinesin motor domain during purification. While biochemical studies have shown a length-dependency with respect to ATP hydrolysis rates for *Drosophila* kinesin [46], the consistency in hydrolytic rates between the native kinesin and kinesin-scFv support the notion of preserved catalytic efficiency. In addition, retained functionality has also been reported for fusion proteins consisting of a human conventional kinesin and the green fluorescent protein [47]. Further characterization to determine the percentage of active kinesin-scFV

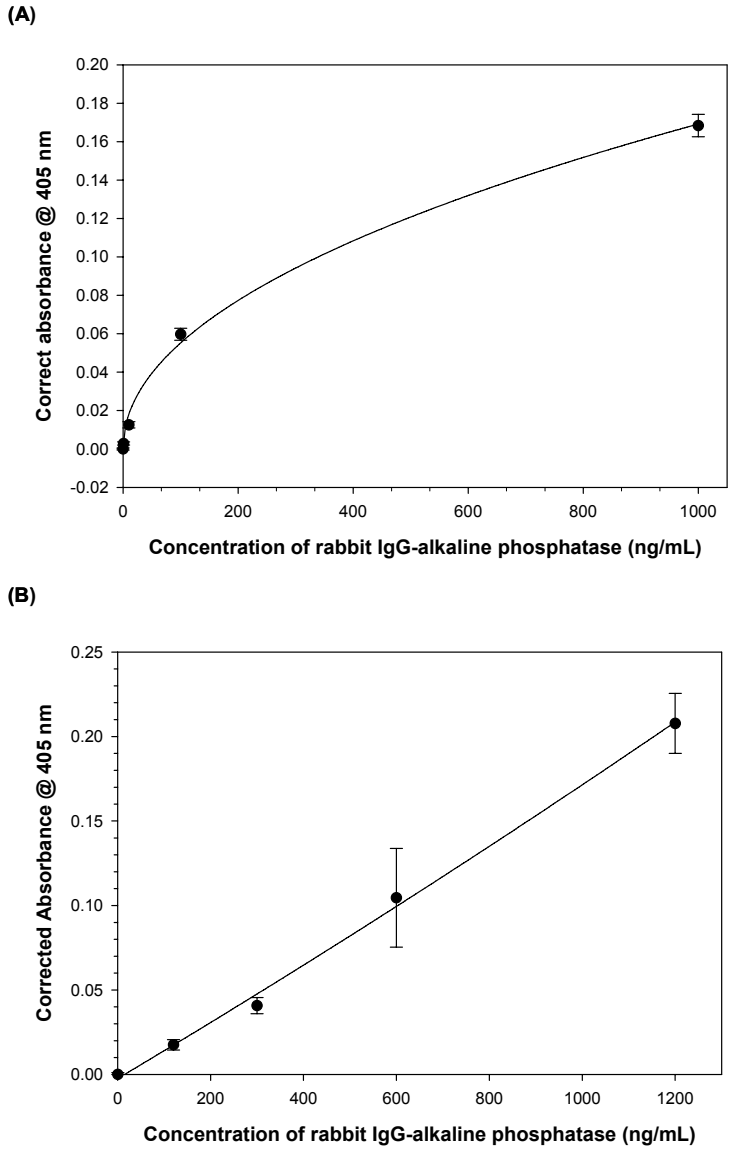

Figure 4: Standard curves for the detection of rabbit immunoglobulin G (IgG)-alkaline phosphatase by the kinesin-scFV fusion protein using two modified ELISAs. In the first assay, kinesin-scFv was bound to microtiter plates using anti-kinesin antibodies (**A**). In the second assay, kinesin-scFv was bound to microtubules present in the microtiter plate wells (**B**).

and the specific activity (i.e., turnover rate of active motors) is necessary to further understand the effects of adding the scFv to the kinesin tail.

The kinesin-scFv also retained the antigen binding and selectivity intrinsic to the anti-rabbit scFv. In both modified ELISAs, a dose-response was observed across the range of conjugated rabbit IgG concentrations (Fig. 4). Significant differences between control and dilutions of the rabbit IgG conjugated were observed by ANOVA ($P < 0.001$). In the

first ELISA, binding of rabbit IgG was detectable at levels as low as 10 ng/mL (Fig. 4A; $P < 0.001$), confirming preserved scFv functionality. However, the ability of the kinesin-scFv to bind microtubule filaments was not tested in this assay. The functionality of both the kinesin and scFv were evaluated in the second ELISA-based procedure. Binding of kinesin-scFv to the microtiter plates was facilitated through microtubules that had been bound to the surface of the plate though anti-tubulin antibodies. Binding of rabbit IgG by the kinesin-scFv was detected at concentrations of 120 ng/mL and greater (Fig. 4B; $P < 0.001$). Together these assays demonstrate the preserved antigenic selectivity of the scFv as well as the microtubule-binding affinity of the kinesin motor domain.

The rationale for introducing the anti-rabbit IgG scFv was to create a generalized platform for functionalizing kinesin with analyte-selective receptors. Polyclonal antisera is produced in rabbits, and widely applied in immunological assays for detection of analytes. The affinity of the anti-rabbit IgG scFv for the constant region of rabbit IgG enables the attachment of antibodies for a wide array of cellular analytes. Thus, construction of the kinesin-scFv specific against rabbit IgG enables the rapid construction of a library of analyte-selective kinesins through the simple binding of a target-selective IgG raised in rabbits.

4.0 Harvesting intact microtubule networks

Kinesin motor proteins have been shown to transport a wide range of micro- and nano-scale particles along microtubule filaments bound to synthetic surfaces [48, 49]. While significant efforts have been made on fabricating microtubule networks in artificial systems [50-52], only sparse two-dimensional arrays have been achieved to date, and do not mimic the natural, three-dimensional architectures found in living systems. It was hypothesized that the existing microtubule network within a cell could be harvested, and serve as a nanoscale scaffold for evaluating and exploiting three-dimensional *in vitro* transport by kinesin motor proteins.

Materials & Methods

Harvesting microtubules from HeLa and B35 cells

Human liver (HeLa) and rat neuronal (B35) cell lines were obtained from the American Type Culture Collection (ATTC), and cultivated at 37ºC in Dulbecco's modified Eagle's medium with 10% fetal bovine serum (5% CO_2). Cell cultures were grown to 80-100% confluency on glass coverslips in 6-well culture plates. Coverslips were gently washed with phosphate buffered saline (1x PBS) warmed to room temperature. For the methanol-based fixation method, coverslips were incubated with extraction buffer (BRB80 + 4 mM EGTA + 0.5% Taxol + ATP [1mM-100mM]) for 30 sec, fixed with cold methanol for 3 min, and subsequently air dried. For glutaraldehyde fixation, coverslips were incubated in microtubule stabilizing buffer (BRB80 + 4 mM EGTA + 0.5% Taxol) for 30 sec, fixed with 0.5% glutaraldehyde for 10 min at 25ºC, washed with fresh buffer, and air dried.

Microtubule networks were fluorescently stained using either anti-tubulin antibodies or BODIPY® FL paclitaxel (Invitrogen Corp). In the first method, coverslips were rehydrated with Tris-buffered saline (1x TBS) with 0.1% Triton X-100, and incubated with a 1:100 dilution of mouse anti-αβ tubulin (diluted in TBS + 0.1% Triton X-100 + 2% BSA) for 15-120 min in the dark at 25ºC. Coverslips were then washed three times with TBS, and a 1:100 dilution of Alexa Fluor® 488 goat anti-mouse antibody (diluted in TBS + 0.1% Triton X-100 + 20 mg/mL BSA) was added for 15-60 min in the dark at 25ºC. Stained microtubule networks were washed three times with TBS, and mounted on glass slides using Cytoseal (Richard Allan Scientific). For the second method, the dried coverslips were rehydrated with a 10 μM solution of BODIPY® FL paclitaxel in BRB80, and incubated for 15 min in the dark at 25ºC. Excess solution was wicked from the coverslip using filter paper, and coverslips were allowed to air dry. The dried coverslip were then used to create a flow cell in which a 10 μM solution of BODIPY® FL paclitaxel in BRB80 was infused in order to maintain fluorescence of the microtubule networks.

In vitro *motility assays on microtubule networks*

The ability of the harvested microtubule networks to support kinesin-based transport was evaluated using a bead-based motility assay [48, 49]. Microtubule networks were incubated with 10 μM solution of BODIPY® FL paclitaxel for 15 min at 25ºC. Coverslips were then allowed to dry, and used to construct flow cells. Silica (200 and 500 nm diameter) and fluorescent, carboxylate-modified polystyrene (200 nm diameter) spheres were washed with BRB80 to remove excess surfactant, and coated with a 4 mg/mL solution of casein. Suspensions were sonicated for 5 min, and incubated at 4ºC for 1-2 hrs with gentle shaking. Casein-coated spheres were then functionalized with a five-fold monolayer coverage of *Drosophila* kinesin at 4ºC for 1 hr. Nanocrystal quantum dots (e.g., carboxyl Qdot®525, Invitrogen, Corp) were also functionalized with kinesin using this protocol. Kinesin-coated spheres and quantum dots were infused into flow cells, and movement was evaluated by epifluorescence microscopy and capturing time-lapse images using a CCD camera.

Results & Discussion

Epifluorescence microscopic evaluation of the fixed microtubule networks demonstrated the ability to harvest intact microtubule networks from HeLa cells using both glutaraldehyde and methanol fixation methods (Fig. 5). Similar results were obtained for B35 rat neuronal cells (*not shown*). While both methods successfully isolated microtubule networks, methanol fixation was superior based on the high fluorescence background observed with glutaraldehyde (Fig. 5C). Quenching reagents may be used in the future to reduce this background fluorescence, but require additional, time-intensive processing steps. Together these methodologies represent a key enabling technology for this project as well as a range of nanotechnological applications. More specifically, the ability to transport nanoscale cargo in three-dimensions greatly enhances the application of kinesin transport systems that are currently limited to planar systems [49-51, 53]. These microtubule networks can be used to study the kinetic rates of

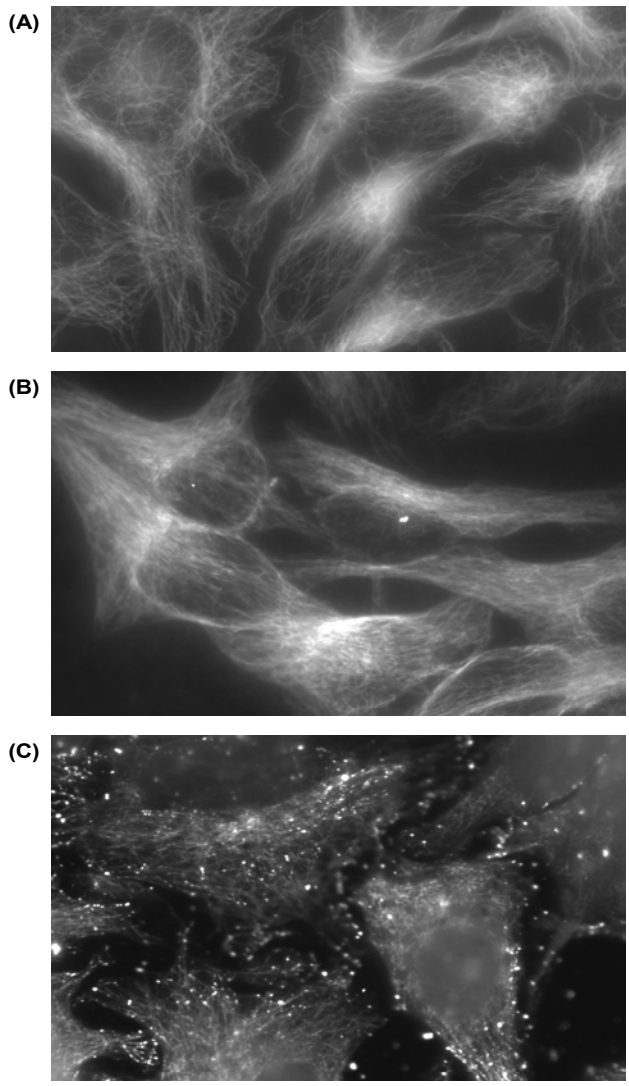

Figure 5: Fluorescence micrographs of intact microtubule networks isolated from HeLa cells using 0.5% methanol (**A**), 1% methanol (**B**), and 0.5% glutaraldehyde (**C**). Microtubules were stained with taxol.

transport and analyte capture, on which models can be developed to predict functionality in live cells. In addition, the cell's microtubule architecture can be applied to hybrid nanoscale system as a three-dimensional transport network that may be used to synthesize structured materials.

Attachment of kinesin-coated quantum dots, and silica and polymer spheres to microtubules was observed by fluorescence microscopy (Fig. 6); movement, however, was not demonstrated for microtubule networks prepared by either fixation method. Control experiments demonstrated the ability of kinesin-coated silica spheres to move

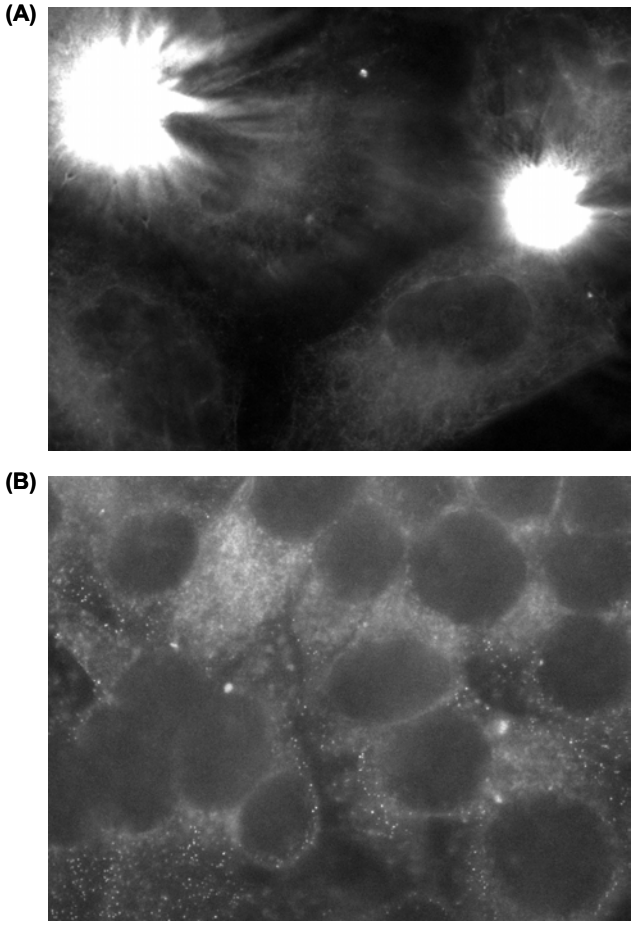

Figure 6: Fluorescence photomicrograph showing the attachment of kinesin-coated silica spheres (**A**) and quantum dots (**B**) to fluorescently labeled microtubule networks harvested from HeLa cells.

along polymerized microtubules, confirming the integrity of the kinesin and assay components. Kinesin-based transport of quantum dots was not verified in control experiments. A number of factors could have potentially limited kinesin function, including the presence of microtubule-associated proteins, excessive crosslinking of tubulin molecules, and increased stiffness of the microtubule filaments. Glutaraldehyde crosslinking of microtubules has been shown to adversely affect kinesin-based transport that is related to the reaction time and crosslinker concentration [54, 55]. However, the glutaraldehyde concentration used for harvesting the microtubule networks was below the critical threshold shown to inhibit kinesin motility. The presence of microtubule associated proteins (MAPs) may also have affected kinesin movement on harvest microtubule networks. Recently, kinesin-based transport of nanocrystal quantum dots was demonstrated [56], which suggests that modified kinesin constructs can successfully move *in vivo* along MAP-coated microtubules. A reduction in the *in vitro* motility

velocity, but not processivity of the kinesin-coated quantum dots, was demonstrated along microtubule fibers that had been treated with non-functional kinesin mutants demonstrated [57]. Thus, steric interference due to MAPs or indigenous kinesin proteins may have affected the transport of kinesin-coated spheres and quantum dots on the harvested microtubule networks. New methods of functionalizing spheres and quantum dots using biotinylated kinesin [53, 56, 57] are currently being evaluated with respect to facilitating transport. Further investigation in the nature of the observed inhibition is fundamental to the future application of these microtubule networks for nanotechnological applications.

5.0 Conclusions

While significant efforts have been placed on applying kinesin-based transport system for nanotechnological application [28-30], this project explored nanoscale engineering of kinesin motor proteins as a means of manipulating active transport within living cells. To this end, a chimeric, fusion protein consisting of kinesin and an antibody fragment (i.e., scFv) were successfully produced through a bacterial expression system. The kinesin-scFv retained both catalytic and antigenic functionality, enabling selective capture and transport of target antigens. Successful isolation of intact microtubule networks from two distinct cell types was also demonstrated, and will provide a platform for inferring the ability of kinesin-scFv to function *in vivo*. Such networks may also serve as a three-dimensional scaffold for evaluating and exploiting kinesin-based transport for nanotechnological applications.

6.0 References

1. Howard, J., *Mechanics of motor proteins and the cytoskeleton*. 2001, Sunderland: Sinauer Associates, Inc. 367.
2. Vale, R.D. and R.J. Fletterick.1997."The design plan of kinesin motors." *Annu. Rev. Cell Dev. Biol.* **13**: p. 745-777.
3. Vale, R.D. and R.A. Milligan.2000."The way things move: Looking under the hood of molecular motor proteins." *Science*. **288**(5463): p. 88-95.
4. Alberts, B., A. Johnson, J. Lewis, M. Raff, K. Roberts, and P. Walter, *The Molecular Biology of the Cell*. 4th ed. 1989, New York: Garland Science, Inc. 1462.
5. Sellers, J.R.2000."Myosins: a diverse superfamily." *Biochim. Biophys. Acta-Mol. Cell Res.* **1496**(1): p. 3-22.
6. Irving, M., G. Piazzesi, L. Lucii, Y.B. Sun, J.J. Harford, I.M. Dobbie, M.A. Ferenczi, M. Reconditi, and V. Lombardi.2000."Conformation of the myosin motor during force generation in skeletal muscle." *Nat. Struct. Biol.* **7**(6): p. 482-485.
7. Vale, R.D.1999."Millennial musings on molecular motors." *Trends Biochem.Sci.* **24**(12): p. M38-M42.
8. Muresan, V., C.P. Godek, T.S. Reese, and B.J. Schnapp.1996."Plus-end motors override minus-end motors during transport of squid axon vesicles on microtubules." *J. Cell Biol.* **135**(2): p. 383-397.
9. Rustom, A., R. Saffrich, I. Markovic, P. Walther, and H.-H. Gerdes.2004."Nanotubular highways for intercellular organelle transport." *Science*. **303**(5660): p. 1007-1010.

10. Lehmler, C., G. Steinberg, K. Snetselaar, M. Schliwa, R. Kahmann, and M. Bolker.1997."Identification of a motor protein required for filamentous growth in Ustilago maydis." *EMBO J.* **16**(12): p. 3464-3473.
11. Haimo, L. and C. Thaler.1994."Regulation of organelle transport - Lessons from color-change in fish." *BioEssays*. **16**(10): p. 727-733.
12. Maniak, M.2003."Organelle transport: A park-and-ride system for melanosomes." *Curr. Biol.* **2**(13): p. R917-R919.
13. Rodionov, V.I., A.J. Hope, T.M. Svitkina, and G.G. Borisy.1998."Functional coordination of microtubule-based and actin-based motility in melanophores." *Curr. Biol.* **8**: p. 165-168.
14. Satir, P.2006."Introduction to primary cilia." *FASEB J.* **20**(4): p. A436-A437.
15. Nédélec, F., T. Surrey, and A.C. Maggs.2001."Dynamic concentration of motors in microtubule arrays." *Phys. Rev. Lett.* **86**(14): p. 3192-3195.
16. Surrey, T., F. Nédélec, S. Leibler, and E. Karsenti.2001."Physical properties determining self-organization of motors and microtubules." *Science*. **292**: p. 1167-1171.
17. Koster, G., M. VanDuijn, B. Hofs, and M. Dogterom.2003."Membrane tube formation from giant vesicles by dynamic association of motor proteins." *Proc. Natl. Acad. Sci. USA*. **100**(26): p. 15583-15588.
18. Carter, N. and R. Cross.2005."Mechanics of the kinesin step." *Nature*. **435**: p. 308-312.
19. Svoboda, K., C.F. Schmidt, B.J. Schnapp, and S.M. Block.1993."Direct observation of kinesin stepping by optical trapping interferometry." *Nature*. **365**(6448): p. 721-7.
20. Asbury, C.L., A.N. Fehr, and S.M. Block.2003."Kinesin moves by an asymmetric hand-over-hand mechanism." *Science*. **302**(5653): p. 2130-2134.
21. Yildiz, A., M. Tomishige, R.D. Vale, and P.R. Selvin.2004."Kinesin walks hand-over-hand." *Science*. **303**(5658): p. 676-678.
22. Coy, D.L., M. Wagenbach, and J. Howard.1999."Kinesin takes one 8-nm step for each ATP that it hydrolyzes." *J. Biol. Chem.* **274**(6): p. 3667-3671.
23. Schnitzer, M.J. and S.M. Block.1997."Kinesin hydrolyses one ATP per 8-nm step." *Nature*. **388**(6640): p. 386-390.
24. Visscher, K., M.J. Schnitzer, and S.M. Block.1999."Single kinesin molecules studied with a molecular force clamp." *Nature*. **400**(6740): p. 184-189.
25. Dennis, J.R., J. Howard, and V. Vogel.1999."Molecular shuttles: directed motion of microtubules along nanoscale kinesin tracks." *Nanotechnology*. **10**(3): p. 232-236.
26. Hess, H.2006."Self-assembly driven by molecular motors." **2**(8): p. 669-677.
27. Hess, H.2006."Materials science - Toward devices powered by biomolecular motors." *Science*. **312**(5775): p. 860-861.
28. Hess, H. and G. Bachand.2005."Biomolecular motors." *Mater. Today*. **8**(12): p. 22-29.
29. Hess, H., G.D. Bachand, and V. Vogel, *Motor proteins in synthetic materials and devices*, in *Dekker Encyclopedia of Nanoscience and Nanotechnology*, J. Schwarz, C. Contescu, and K. Putyera, Editors. 2004, American Scientific Publishers: New York. p. 2201-2209.
30. Hess, H., G.D. Bachand, and V. Vogel.2004."Powering nanodevices with biomolecular motors." *Chem. Eur. J.* **10**(9): p. 2110-2116.
31. Dohner, K. and B. Sodeik.2004."The role of the cytoskeleton during viral infection." *Curr. Top. Microbiol. Immunol.* **285**: p. 67-108.
32. Marte, B.2001."Vaccinia virus on the move." *Nat. Rev. Mol. Cell Biol.* **2**(11): p. 792.
33. Sodeik, B.2000."Mechanisms of viral transport in the cytoplasm." *Trends Microbiol.* **8**(10): p. 465-472.
34. Biswas, D., K. Itoh, and C. Sasakawa.2003."Role of microfilaments and microtubules in the invasion of INT-407 cells by Campylobacter jejuni." *Microbiol. Immunol.* **47**(6): p. 469-473.

35. Boucrot, E., T. Henry, J.P. Borg, J.P. Gorvel, and S. Meresse.2005."The intracellular fate of Salmonella depends on the recruitment of kinesin." *Science*. **308**(5725): p. 1174-1178.
36. Gouin, E., M.D. Welch, and P. Cossart.2005."Actin-based motility of intracellular pathogens." *Curr. Opin. Microbiol.* **8**(1): p. 35-45.
37. Smith, G.A. and L.W. Enquist.2002."Break ins and break outs: Viral interactions with the cytoskeleton of mammalian cells." *Annu. Rev. Cell Dev. Biol.* **18**: p. 135-161.
38. Smith, G.L., B.J. Murphy, and M. Law.2003."Vaccinia virus motility." *Annu. Rev. Microbiol.* **57**: p. 323-342.
39. Dohner, K., A. Wolfstein, U. Prank, C. Echeverri, D. Dujardin, R. Vallee, and B. Sodeik.2002."Function of dynein and dynactin in herpes simplex virus capsid transport." *Mol. Biol. Cell*. **13**(8): p. 2795-2809.
40. Douglas, M.W., R.J. Diefenbach, F.L. Homa, M. Miranda-Saksena, F.J. Rixon, V. Vittone, K. Byth, and A.L. Cunningham.2004."Herpes simplex virus type 1 capsid protein VP26 interacts with dynein light chains RP3 and Tctex1 and plays a role in retrograde cellular transport." *J. Biol. Chem.* **279**(27): p. 28522-28530.
41. Dohner, K., C.H. Nagel, and B. Sodeik.2005."Viral stop-and-go along microtubules: taking a ride with dynein and kinesins." *Trends Microbiol.* **13**(7): p. 320-327.
42. Smith, G.A., S.P. Gross, and L.W. Enquist.2001."Herpesviruses use bidirectional fast-axonal transport to spread in sensory neurons." *Proc. Natl. Acad. Sci. USA*. **98**(6): p. 3466-3470.
43. Albrecht, H., G.L. DeNardo, and S.J. DeNardo.2006."Monospecific bivalent scFv-SH: Effects of linker length and location of an engineered cysteine on production, antigen binding activity and free SH accessibility." *J. Immunol. Methods*. **310**(1-2): p. 100-116.
44. Vaccaro, P., E. Pavoni, G. Monteriu, P. Andrea, F. Felici, and O. Minenkova.2006."Efficient display of scFv antibodies on bacteriophage lambda." *J. Immunol. Methods*. **310**(1-2): p. 149-158.
45. Al-Bassam, J., Y. Cui, D. Klopfenstein, B.O. Carragher, R.D. Vale, and R.A. Milligan.2003."Distinct conformations of the kinesin Unc104 neck regulate a monomer to dimer motor transition." *Proc. Natl. Acad. Sci. USA*. **24**(163): p. 743-753.
46. Moyer, M.L., S.P. Gilbert, and K.A. Johnson.1996."Purification and characterization of two monomeric kinesin constructs." *Biochemistry*. **35**(20): p. 6321-6329.
47. Seitz, A., H. Kojima, K. Oiwa, E.M. Mandelkow, Y.H. Song, and E. Mandelkow.2002."Single-molecule investigation of the interference between kinesin, tau and MAP2c." *EMBO J.* **21**(18): p. 4896-4905.
48. Böhm, K.J., J. Beeg, G.M. zu Horste, R. Stracke, and E. Unger.2005."Kinesin-driven sorting machine on large-scale microtubule arrays." *IEEE Trans Adv Pack*. **28**(4): p. 571-576.
49. Limberis, L. and R.J. Stewart.2000."Toward kinesin-powered microdevices." *Nanotechnology*. **11**(2): p. 47-51.
50. Limberis, L., J.L. Madga, and R.J. Stewart.2001."Polarized alignment and surface immobilization of microtubules for kinesin-powered nanodevices." *Nano Lett.* **1**(5): p. 277-280.
51. Muthukrishnan, G., C.A. Roberts, Y.C. Chen, J.D. Zahn, and W.O. Hancock.2004."Patterning surface-bound microtubules through reversible DNA hybridization." *Nano Lett.* **4**(11): p. 2127-2132.
52. Böhm, K.J., R. Stracke, P. Muhlig, and E. Unger.2001."Motor protein-driven unidirectional transport of micrometer-sized cargoes across isopolar microtubule arrays." *Nanotechnology*. **12**(3): p. 238-244.
53. Muthukrishnan, G., B.M. Hutchins, M.E. Williams, and W.O. Hancock.2006."Transport of

semiconductor nanocrystals by kinesin molecular motors." *Small*. **2**(5): p. 626-630.
54. Boal, A., H. Tellez, S. Rivera, N. Miller, G. Bachand, and B. Bunker.2006."The stability and functionality of chemically crosslinked microtubules." *Small*. **2**(6): p. 793-803.
55. Turner, D., C. Chang, K. Fang, P. Cuomo, and D. Murphy.1996."Kinesin movement on glutaraldehyde-fixed microtubules." *Anal. Biochem.* **242**(1): p. 20-25.
56. Courty, S., C. Luccardini, Y. Bellaiche, G. Cappello, and M. Dahan.2006."Tracking individual kinesin motors in living cells using single quantum-dot imaging." *Nano Lett.* **6**(7): p. 1491-1495.
57. Seitz, A. and T. Surrey.2006."Processive movement of single kinesins on crowded microtubules visualized using quantum dots." *EMBO J*. **25**(2): p. 267-277.

Distribution

1	MS 1413	G.D. Bachand, 8331
1	MS1413	A. Carroll-Portillo, 8331
1	MS 9054	T.A. Michalske, 8300
2	MS 9018	Central Technical Files 89444
2	MS0899	Technical Library, 4536